Mineral Spectroscopy: A Tribute to Roger G. Burns
© The Geochemical Society, Special Publication No. 5, 1996
Editors: M. D. Dyar, C. McCammon and M. W. Schaefer

A comprehensive Mössbauer study of highly-substituted aluminum maghemite*

G. M. da Costa,[1,2] Ch. Laurent,[3] E. De Grave,[1] and R. E. Vandenberghe[1]
[1]Laboratory of Magnetism, Department of Subatomic and Radiation Physics, University of Gent, Proeftuinstraat 86, B-9000, Belgium
[2]On leave from Departamento de Química, Universidade Federal de Ouro Preto, Ouro Preto, MG, Brazil
[3]Laboratoire de Chimie des Materiaux Inorganiques, Universite Paul Sabatier, Toulouse Cedex, France

Abstract—Synthetic Al-substituted maghemite samples, γ-$(Al_yFe_{1-y})_2O_3$, with $y = 0$, 0.10, 0.15, 0.22, 0.37, 0.55 and 0.66, were prepared from an oxalate precursor. The samples were studied by Mossbauer spectroscopy (MS) at 4.2 K in an applied magnetic field of 60 kOe, as well as at 8 K and in the range 80 K to 475 K at steps of 30 K in zero-field. Powder X-ray diffraction (XRD) and transmission electron microscopy (TEM) were applied as well. The particles are more or less spherical and the sizes determined from the XRD experiments decreased from approximately 80 nm for the Al-free sample to about 8 nm in the highly substituted samples. At 4.2 K the dependence of the hyperfine fields was found to be $H_{hf,A} = (520 - 30y)$ kOe and $H_{hf,B} = (531 - 26y)$ kOe, suggesting that the Al ions are located on both sites. Further information on the Al distribution was obtained from the relative areas, which are in agreement with a 50/50 distribution, *i.e.*, half of the Al on the tetrahedral sites and half on the octahedral ones. The canting angles were found to be Al-dependent, and for high substitutions the moments seem to be no longer collinear. The temperature dependence of the A- and B-site hyperfine fields could be reproduced using molecular field theory assuming an antiparallel spin configuration. The exchange integrals were found to be $J_{AA} = -18$ K, $J_{AB} = -27$ K and $J_{BB} = -4$ K. The Curie temperature (T_C) decreased with Al as $T_C = (948 - 990y)$ K for $y < 0.22$. The A-site hyperfine field becomes larger than that of the B site in the vicinity of 300 K, and this crossing temperature depends on the Al content. The variation of the center shifts with T was interpreted in terms of the Debye model, but the derived characteristic Mossbauer temperature and intrinsic isomer shift bear no relation to Al.

INTRODUCTION

The discovery of the Mössbauer effect, and in particular of the existence of that effect in ^{57}Fe, has created a new incentive for the study of both synthetic and natural Fe-containing minerals. The use of this technique for the study of soils and sediments has been reviewed on a regular basis by Bowen and co-authors (Bowen, 1979; Bowen and Weed 1984; Bowen *et al.,* 1993). Since such systems are normally composed of mixtures of various and mostly poorly crystalline compounds, emphasis has been given to the correct characterization of the pure constituents. Another fact that has caught the attention of many researchers is the possibility that some of these natural compounds contain foreign cations isomorphically substituting for iron. Thus, the effects of both poor crystallinity and isomorphic substitution have been extensively studied, especially in the case of hematite (α-Fe_2O_3) and goethite (α-FeOOH), which are known to be present in almost all kinds of soils. Nevertheless, it was realised in recent years that another iron oxide, maghemite (γ-Fe_2O_3), also occurs in many tropical soils (Schwertmann and Fechter, 1984). This mineral, occurring with or without magnetite (Fe_3O_4) is believed to be the main one responsible for the magnetic character of such soils.

Maghemite is a cation-deficient spinel with 21 1/3 1/3 Fe^{3+} ions distributed among eight tetrahedral (A) and sixteen octahedral (B) sites of the unit cell; $2\frac{2}{3}$ sites per unit cell are vacant. It is commonly represented by the formula $(Fe)[Fe_{5/3}\square_{1/3}]O_4$, where ( ) denotes tetrahedral sites, [ ] octahedral sites and □ vacancies. However, it was reported that the vacancies can occur on both A and B sites simultaneously (Armstrong, 1966; Annersten and Hafner, 1973; Haneda and Morrish, 1977a). Well crystallized maghemite further exhibits a 1 : 5 ordering of □ and Fe within the octahedral sublattice, giving rise to X-ray reflections which are normally not observed for a cubic spinel structure (Van Oosterhout and Rooijmans, 1958). This ordering of the vacancies is size-dependent, and for particles smaller than approximately 20 nm it ceases to exist (Haneda and Morrish, 1977b).

Little is known about the influence of isomorphic substitution on the properties of maghemite, and

---

* Contribution No SSF95-03-02 from the Department of Subatomic and Radiation Physics, University of Gent, Belgium.

only very recently a systematic study of the effect of both Al and poor crystallinity was reported by this research group. Nano-sized maghemite and Al-maghemites prepared by thermal treatment of lepidocrocite (γ-FeOOH) containing up to 18 mole % Al, and hereafter referred to as ML samples, were studied by da Costa *et al.* (1994a, 1995a). The first paper emphasizes the difficulties in analysing the zero-field Mössbauer spectra (ZFMS) of such samples. In addition, the results of the spectra collected at 4.2 K under an applied field of 60 kOe (AFMS) were presented and from them it was concluded that 10 mole % may be a solubility limit for Al in the maghemite structure. This proposition had been suggested earlier by Wolska and Schwertmann (1989) and Bowen *et al.* (1994), but Gillot and Rousset (1990) claimed that up to 66 mole % could be incorporated in maghemite samples prepared from an oxalate precursor. The second paper (da Costa *et al.,* 1995a) dealt with the results derived from the spectra collected at 8 K, and between 80 K and 475 K (steps of 25 K) without an applied field. Several important parameters such as the blocking temperatures, average hyperfine fields at 8 K, A- and B-site quadrupole splittings, and the so-called *Characteristic Mössbauer temperature,* have been obtained.

Relatively well-crystallized Al-maghemites prepared from Al-hematites, hereafter referred to as M samples, were also examined by Bowen *et al.* (1994) and da Costa *et al.* (1994b, 1995b). One of the main objectives of these latter studies was to clarify an unacceptably wide scatter in the Mössbauer data concerning non-substituted γ-Fe_2O_3 as reported in literature. It was shown from the AFMS, both at 4.2 K as well as at 275 K, that the A-site center shift is on the average 0.12 mm/s smaller than that of the B site, regardless of temperature and Al content. This important finding enabled the authors to correctly fit the ZFMS collected at 8 K, and between 80K and 475 K at steps of 25 K (da Costa *et al,* 1995b). Thus, both the *Characteristic Mössbauer temperature* and the intrinsic isomer shift for the B site showed an increase with increasing the Al content, at least up to 10 mole %. The temperature dependence of the A- and B-sites hyperfine fields could be satisfactorily reproduced using the molecular-field theory assuming an antiparallel spin configuration. The exchange integrals were found to be $J_{AB} = -25$ K, $J_{AA} = -18$ K, and $J_{BB} = -3$ K. The Curie temperature for the Al-free sample was determined to be 930 K, and it decreased with increasing Al content.

To the best of the authors' current knowledge only two other papers dealing with the MS of Al-maghemites have been published. In one of them, four samples containing between zero and 11 mole % Al were prepared by oxidation of magnetite (de Jesus Filho *et al.,* 1993). The cell parameter was reported to decrease from 0.8337 nm to 0.8292 nm for the 11 mole % sample. Magnetization measurements gave a lower than expected value for the spontaneous magnetization, and to explain this result the authors proposed the existence of spin canting on B sites only, and that the vacancies are distributed over the two sites. The second paper was published by Bowen *et al.* (1994), and concerns Al-maghemites prepared by several thermal treatments of a mixture of sucrose and Al-hematites containing up to 15 mole % Al. Both vacancies and Al were found to occupy the B sites exclusively.

As mentioned above, the solubility limit of Al in maghemite is still a matter of some dispute. In an attempt to solve this question, Mössbauer spectra of several highly-substituted samples have been collected at 4.2 K in an applied-field of 60 kOe, and also at 8 K and between 80 K and 475 K at steps of 30 K in zero field. These samples were prepared by the method reported by Rousset and Paris (1972). In what follows it will be demonstrated that up to 66 mole % of Al can indeed be incorporated into the maghemite lattice.

EXPERIMENTAL PROCEDURES

All samples were prepared according to the method originally proposed by Rousset and Paris (1972). It consists of several thermal treatments of co-precipitated Fe-Al oxalate precursors. Initially the mixed oxalates $(NH_4)_3[Fe_{1-x}Al_x(C_2O_4)_3] \times 3H_2O$, with $0 < x < \frac{2}{3}$, are decomposed in air at 400°C. The materials thus obtained are subjected to reduction in a H_2-H_2O atmosphere in order to produce magnetite. Finally, oxidation was carried-out in air at 210°C. Samples are code-named DG00, DG10, DG15, DG22, DG37, DG55 and DG66, where the numbers refer to the mole % Al in γ-$(Fe_{1-y}Al_y)_2O_3$, as determined by atomic absorption.

Powder X-ray diffraction (XRD) patterns were obtained using a Philips diffractometer with CoKα radiation and a graphite monochromator. The scans were done in the range of 15–80° (2θ) at a speed of $\frac{1}{4}$° min^{-1}, and the reflected intensities were recorded in a multichannel analyser. The diffractograms were fitted with a sum of pseudo-Lorentzians, two for each peak in order to account for the Kα1 and Kα2 radiation. Mean crystallite dimensions (MCD) along the [110] and [311] lattice directions were estimated from the full widths at half maximum using Scherrer's equation with K = 0.9. Lattice parameters were determined by the Nelson-Riley extrapolation method (Klug and Alexander, 1974). An internal standard (Si) was used in some runs.

Zero-field Mössbauer spectra were collected at 8 K and between 80–475 K in steps of 30 K. An external field of 60 kOe parallel to the direction of the incident γ-rays was applied at 4.2 K for all samples, and at intermediate temperatures for sample DG66. All center shifts are

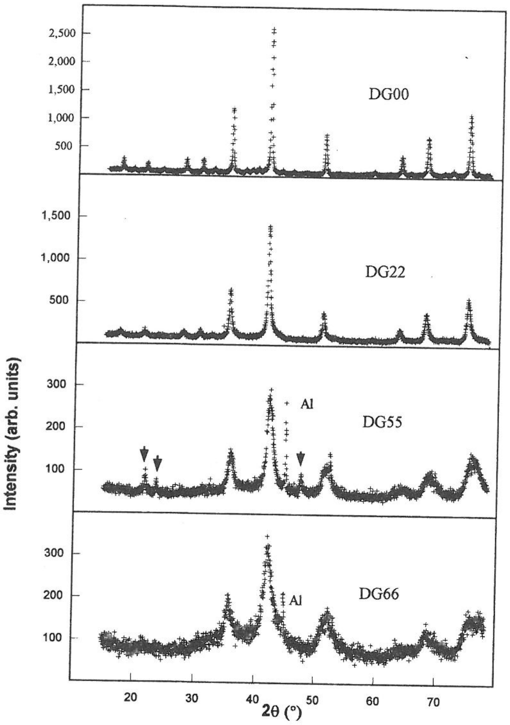

FIG. 1. X-ray diffraction patterns of maghemite (DG00) and Al-substituted maghemites (DG22, DG55 and DG66). Some superstructure lines are clearly visible in samples DG00 and DG22. Peaks marked with an arrow in sample DG55 are due to bayerite, while peaks marked as Al are due to the sample holder.

quoted relative to metallic iron. More details about the experimental set-up can be found elsewhere (DA COSTA *et al.*, 1994b). The overall number of spectra exceeds 100 and not all data will be presented here, but are available upon request.

Transmission electron microscopy (TEM) was performed with a JEOL 200CX operating at 200 kV. The powders were ultrasonically dispersed in ethanol and a drop of the dispersion was deposited onto a copper grid coated with a collodion film.

RESULTS AND DISCUSSION

X-ray diffraction

The XRD of samples DG00, DG22, DG55 and DG66 are shown in Fig. 1. Some superstructure lines are evident in the diffractograms of samples DG00, DG10, DG15 and DG22, indicating that for these compositions the vacancies are ordered on the B sites. For higher Al contents the lines become increasingly broader, probably due to the combined effects of small-particle sizes and high amounts of aluminum. There are three reflections for DG55 which do not correspond to a spinel phase. They were identified as belonging to bayerite ($Al_2O_3 \times 3H_2O$). Furthermore, it is to be noted that for DG66 the background in the region of 20–40° seems to be higher than outside that region, perhaps indicating the presence of another phase. One possible candidate is ferrihydrite (or most probably Al-ferrihydrite), which has the main peak around 40°. This substance is known to be very poorly crystallized, giving rise to a characteristic XRD pattern showing only 2 or 6 extremely broad lines (EGGLETON and FITZPATRICK, 1988). Ferrihydrite transforms to hematite by heating at around 300°C, but the stability of Al-ferrihydrite is much higher. For a 16 mole % Al the transformation to hematite occurs at 500°C (CHADWICK *et al.*, 1986). Thus, it is not impossible that sample DG66 contains Al-ferrihydrite as an impurity.

The cell parameters and the particle sizes along the [110] and [311] lattice directions are given in Table 1. Both quantities decrease with increasing Al content. In particular the particle size drastically lowers from the Al-free sample to the 66 mole % sample. The cell parameters listed in Table 1 differ considerably from those reported by GILLOT and ROUSSET (1990), especially for higher substitutions. In order to check for any possible systematic errors, the diffractograms of some samples were also obtained with a Siemens D5000 diffractometer, and the cell parameters derived from these runs are essentially the same as those in Table 1. Thus, the origin of the discrepancy between the present results and those reported in Gillot's paper could not be traced. A plot of cell parameters vs. Al content does not give a straight line, and a possible reason for that might be the smaller

Table 1. Lattice constants (a) and mean crystallite dimensions (MCD) along the [110] and [311] lattice directions. The estimated error on the lattice parameters is 0.0005 nm.

Sample	a (nm)	MCD110 (nm)	MCD311 (nm)
DG00	0.8348	80	60
DG10	0.8337	50	40
DG15	0.8326	35	35
DG22	0.8329	40	30
DG37	0.8341	20	20
DG55	0.8231	10	10
DG66	0.8146	10	5

MCD of the highly substituted samples. This effect was reported to become important in Co ferrites smaller than 20 nm (VANDENBERGHE *et al.*, 1980), and the samples with y > 0.37 have sizes of that order.

TRANSMISSION ELECTRON MICROSCOPY

TEM observations revealed that the DG00, DG10, DG15 and DG22 specimens are very similar to one another. A representative micrograph of these powders is shown in Fig. 2 for sample DG22. The grains are isotropic in shape and their sizes are in the range 25–200 nm. Indexing of the electron microdiffraction patterns (EMD) revealed that all rings belong to a maghemite-type phase. However, some grains form larger, elongated particles as if they were sintered, but the diffraction spots on the EMD patterns of these grains also belong to a maghemite phase. A few agglomerates composed of small black dots in a grey matrix were also observed for DG15. Their EMD pattern shows diffraction rings and spots that could be ascribed to a mixture of maghemite and some unreacted magnetite-type oxide. As for DG55 and DG66, their smaller crystallite sizes are obvious from the TEM micrographs (Fig. 2). These powders are also more heterogeneous than those containing less alumi-

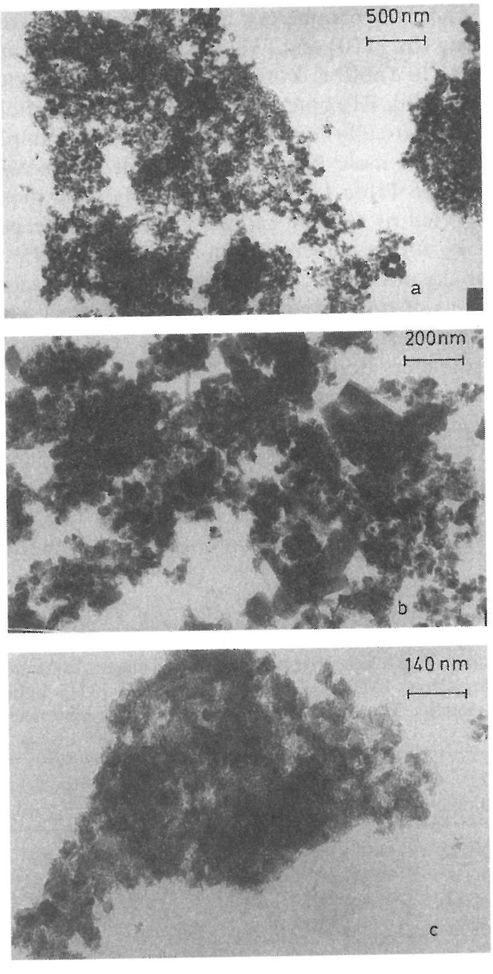

FIG. 2. TEM photographs of samples DG22 (a), DG55 (b) and DG66 (c).

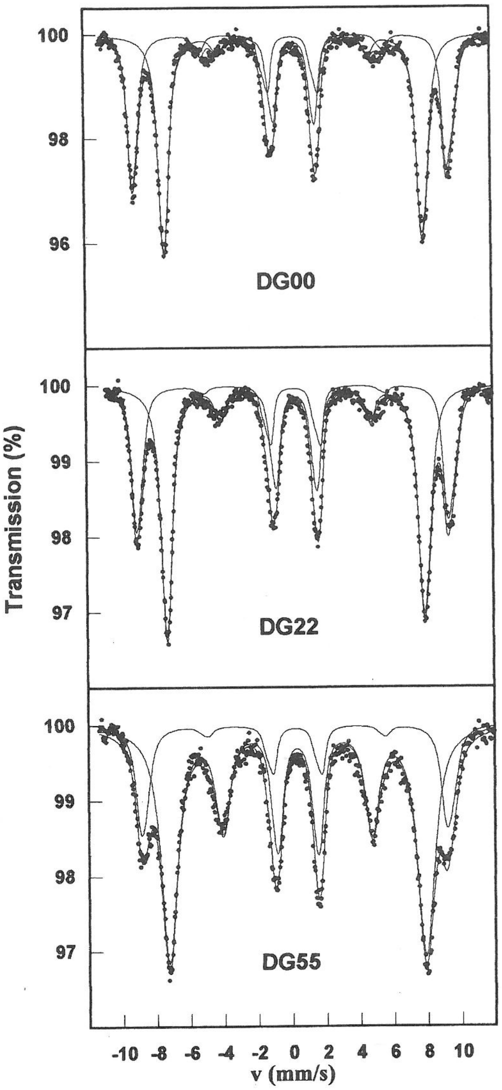

FIG. 3. Mössbauer spectra collected at 4.2 K in an applied field of 60 kOe. Dots represent the experimental data, and full lines represent the calculated subspectra and their sum.

num. For instance, small needle-shaped grains could be observed in some micrographs, especially in DG37 (not shown in Fig. 2). These needles are probably due to maghemite grains that did not yet sinter to a more isotropic shape. Indeed, it is known that there is a threshold temperature at which such a sintering phenomenon occurs, which notably depends on the formation temperature and kinetics of the maghemite phase and on its grain size (ROUSSET *et al.*, 1979). In addition, the micrograph of sample DG55 (Fig. 2) shows the presence of "bottle-shaped" grains. The EMD pattern of such a "bottle" is fairly poor, but the measured distances could match those of $FeAl_2O_4$.

MÖSSBAUER SPECTROSCOPY

Applied-field spectra

Figure 3 shows the Mössbauer spectra at 4.2 K in an applied-field of 60 kOe for samples DG00, DG22 and DG55. These spectra were fitted with two main asymmetric sextet components. The asymmetry is due to the combined effects of random orientation of the hyperfine field with respect to the electric-field-gradient's principal axis and a non-zero dipolar contribution to the hyperfine field (DE GRAVE *et al.*, 1993). For samples DG15 and DG37 a weak hematite component (~3 mole %) had to be included to account for the large broadening of lines 2 and 5 (BOWEN *et al.*, 1994). In AFMS the observed hyperfine field (H_{eff}) is given by the vectorial summation of the applied field (H_{ext}) and the internal field (H_{hf}). The parameters derived from this fit procedure are given in Table 2, and several important conclusions can be reached from them. The averaged difference between the B- and A-site center shifts is 0.12 mm/s, in excellent agreement with the value reported earlier for the M samples. As discussed in detail by DA COSTA *et al.* (1995b), the correct interpretation of the ZFMS of maghemite requires that the difference between the A- and B-site center shifts remains fixed at 0.12 mm/s. This same constraint was applied to analyse the spectra of the present samples.

The presence of lines 2 and 5, which are expected to vanish if the hyperfine fields are completely aligned along the external field (H_{ext}), is a well-documented aspect of the AFMS of maghemite and is due to a canting of the spins with respect to $\vec{H}_{ext}$. There are several propositions in literature to explain the origin of this canting (COEY, 1971; MORRISH *et al.*, 1976; HENDRIKSEN *et al.*, 1994a) and the interested reader is referred to these original papers. In addition, it is still a matter of controversy as to whether or not the A- and B-site moments remain collinear with one another. Some investigators have suggested that the A-site moments are completely aligned with $\vec{H}_{ext}$, while those from the B site are canted (POLLARD, 1990; DE JESUS FILHO *et al.*, 1993). On the other hand it has also been proposed that the moments remain collinear, although canted with respect to H_{ext} (POLLARD and MORRISH, 1987; DE BAKKER *et al.*, 1991). From the relative areas $A_{2,5} : A_{1,6}$ of the middle to outer lines, one can determine the canting angle θ, defined as the angle between $\vec{H}_{hf}$ and H_{ext}, (VANDENBERGHE and DE GRAVE, 1989). The results given in Table 2 for θ_A and θ_B show that for low substitutions ($y < 0.15$) the summation of θ_A and θ_B is close to 180°, indicating that the net moments are likely to be collinear. For higher substitutions there seems to exist a systematic decrease of θ_B with increasing Al content, but not for θ_A. Nevertheless, it cannot be ruled out that the lower intensity of the A-site absorption prevents an accurate determination of the area of lines 2 and 5. On the other hand it is clear that the summation of θ_A and θ_B deviates substantially from 180°, suggesting that the moments are no longer collinear in these highly substituted maghemites.

The inclusion of Al in the structure causes the loss of some exchange paths, hence reducing the

Table 2. Effective hyperfine fields H_{eff} (kOe), hyperfine fields H_{hf} (kOe), canting angles θ (°), center shifts δ (mm/s), full-widths at half maximum of the third and fourth absorption lines (Γ, mm/s) and relative area RA (%) obtained from the spectra collected at 4.2 K in an applied field of 60 kOe. A and B refer to tetrahedral and octahedral sites respectively. Estimated errors are 1 kOe for H_{eff}, 4 kOe for H_{hf}, 5° for θ, and 0.005 mm/s for δ.

Sample	$H_{eff.A}$	$H_{hf.A}$	θ_A	δ_A	Γ_A	RA	$H_{eff.B}$	$H_{hf.B}$	θ_B	δ_B	Γ_B	RA
DG00	577	521	22	0.33	0.34	40	473	530	161	0.45	0.44	60
DG10	575	517	12	0.34	0.42	36	473	530	160	0.45	0.47	64
DG15	572	514	16	0.36	0.31	37	470	527	159	0.49	0.34	63
DG22	572	514	15	0.33	0.37	34	472	527	156	0.45	0.48	66
DG37	567	508	8	0.36	0.44	27	469	521	149	0.48	0.44	73
DG55	560	504	20	0.32	0.43	22	470	517	140	0.42	0.63	78

values of the hyperfine fields. The observed steady decrease in fields (Table 2) can be fitted according to the eqns:

$$H_{hf,A} = (520 - 30y)\ \text{kOe}$$

$$H_{hf,B} = (531 - 26y)\ \text{kOe}$$

BOWEN *et al.* (1994) collected external-field spectra for the M samples ($y \leq 0.15$) and reported a decrease of about 40 kOe per mole of Al for the A-site hyperfine field. In addition, DA COSTA *et al.* (1995b) also indicated a decrease of the same magnitude based on the ZFMS collected at 8 K for the same M series. As for the B sites, any change in H_{hf} remained inconclusive. The fact that for the present maghemites both A- and B-site hyperfine fields decrease with increasing Al content is a strong indication that the Al ions are located on both sites. If there is no substitution on the A sites, the B-site hyperfine field should remain fairly constant because no reduction of supertransfer of spin density from A- to B-site ferric ion would occur.

The above conclusion with respect to the Al distribution is corroborated by the relative A- and B-site area ratios (RA) derived from the AFMS (Table 2). This parameter for the A-site absorption is plotted as a function of Al substitution in Fig. 4, together with values expected on the basis of some specific assumptions. Surprisingly the best overall agreement is not with a random substitution but instead with a 50/50 distribution, *i.e.,* half of the Al entering the tetrahedral sites and half the octahedral sites. For low y values, a random distribution could not be excluded, but for higher substitutions it is clear that a random substitution is grossly in disagreement with the experimental data. As the synthesis of maghemite was carried out at fairly low temperatures, *i.e.,* 210°C, it can be expected that the same cation distribution should exist in the magnetite precursor. Thus, if we represent magnetite as $Fe^{3+}(Fe^{2+}Fe^{3+})O_4$, and consider that the Al ions would replace Fe^{3+} cations, it seems that indeed a random inclusion of Al results in a ratio of 50/50, and not of 37.5/62.5 as predicted by considering the maghemite formula. This Al distribution differs from that derived for the ML samples, in which a random distribution of both Al and vacancies was proposed. However, it is conceivable that the cation distribution depends upon the formation mechanism.

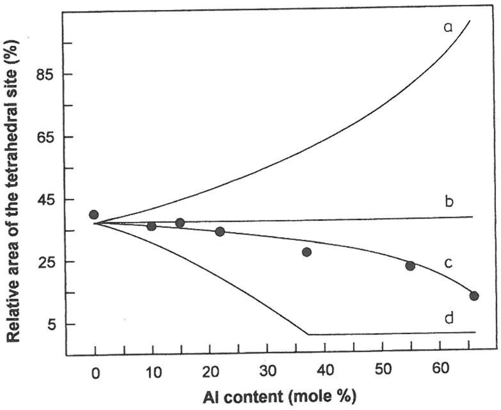

FIG. 4. Theoretical (solid lines) and experimental (dots) tetrahedral area as a function of Al content. The theoretical curves were calculated assuming that the Al ions are located: on B sites (a), distributed at random (b), distributed in a 50/50 ratio (c), and on A sites (d). The experimental data were obtained from the in-field spectra at 4.2 K.

The spectra of sample DG66 at 4.2 K and 55 K, both with and without an external field clearly indicate the existence of an impurity phase in addition to the maghemite (DA COSTA, 1995c). As this impurity tremendously complicates the analysis of the MS, no detailed attention will be paid to this composition.

Zero-field spectra

The ZFMS of samples DG00, DG22 and DG55 at 8 K and 300 K are reproduced in Fig. 5. The spectra of the other samples, as well as those at other temperatures, are similar to those displayed. At 8 K one broad and asymmetric sextet, characteristic for maghemite is obtained. At a given temperature T, depending on y, the spectra of all samples, except DG00, contain an additional doublet, which grows at the expense of the sextet component. This feature is typical for superparamagnetic particles (MØRUP and TOPSØE, 1976), and the appearance of a doublet is expected considering the estimated particle sizes of samples DG37, DG55 and DG66.

Two different approaches to fit the experimental data have been followed. For samples DG00, DG10, DG15 and DG22 the spectra were fitted as a superposition of two asymmetric Lorentzian-sextet profiles (VANDENBERGHE *et al.,* 1994) with three sets of width parameters, equal for A- and B-site subspectra. Thus, lines one and six, two and five, and three and four of each subspectrum were assumed to have the same shape with a high-field (Γ_{HF}) and a low-field (Γ_{LF}) line width. A very important restriction concerns the A-site center shift, which was constrained as $\delta_A = \delta_B - 0.12$ mm/s. Due to the strong overlap of the two patterns some other constraints were imposed: quadrupole shift $\epsilon_Q = 0$ fixed for both sextets, line-

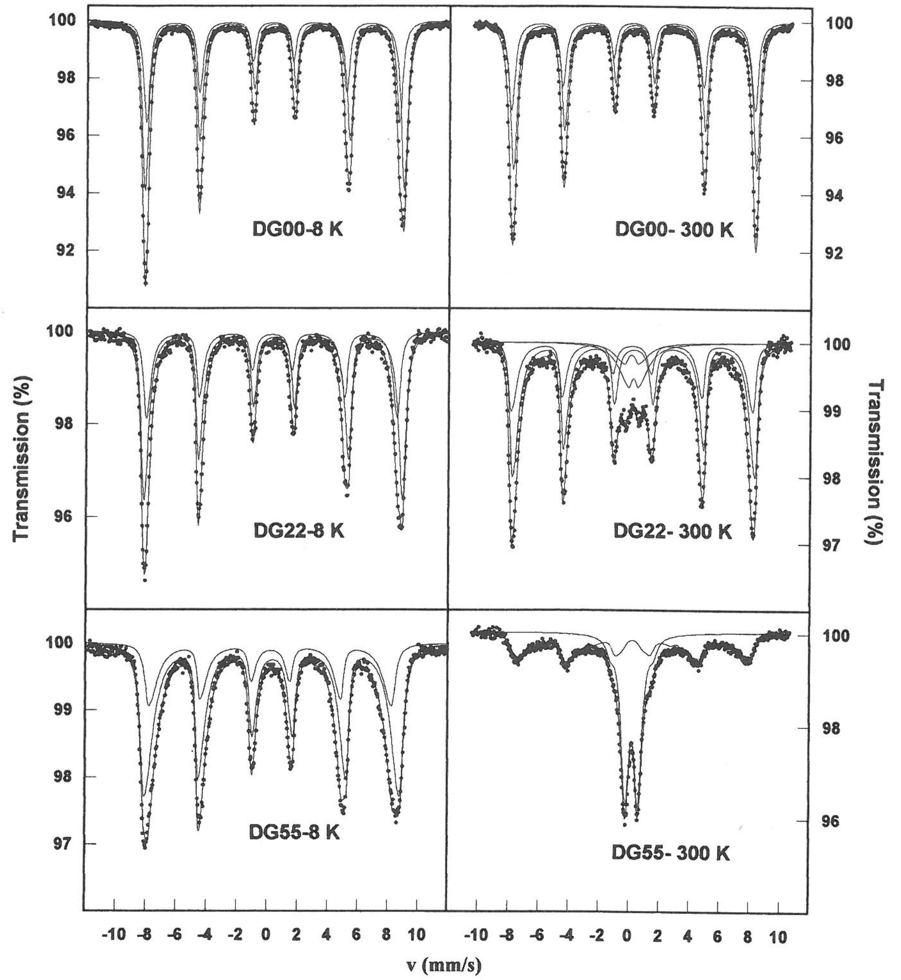

FIG. 5. Zero-field Mössbauer spectra of samples DG00, DG22 and DG55 at 8 K and 300 K. Dots represent the experimental data, and full lines represent the calculated subspectra and their sum.

area ratios fixed at 3 : x : 1, and fixed B- to A-site area fraction as obtained from the external field measurements. Typical iterated values for x were in the range 1.9–2.1. The doublet component was fitted as a superposition of two contributions with different quadrupole splittings, using the same constraints for the isomer shifts and fractional area ratios as listed above for the sextet components (DA COSTA *et al.*, 1995a).

The solid lines in Fig. 5 are the adjusted curves based on the methodology described above (except sample DG55, see below). The agreement between the experimental and fitted spectra is satisfactory. Some numerical results at selected temperatures are presented in Table 3. The ZFMS recorded at 8 K for DG37 and DG55 could be fit in the same manner, and the data are included as well. The agreement between the A- and B-site hyperfine fields at 8 K with the values obtained from the AFMS (4.2 K) is reasonable, and this finding supports the adopted fitting procedure. However, the differences for the B site show more disagreement at high Al contents than for the A site. This is probably related to the fact that as the Al content increases the lines become more asymmetric, and not necessarily in the same amount for the two sites. Some authors have found a much poorer agreement between the hyperfine-field values as obtained with and without an external field (DE BAKKER *et al.*, 1991; HENDRIKSEN *et al.*, 1994b). However, DA COSTA *et al.* (1995b) have demonstrated that this disagreement is an artifact of the fitting procedure the authors applied to analyse

Table 3. Mössbauer parameters obtained from fitting the zero-field spectra of Al-maghemites with two asymmetric-Lorentzian profiles. Γ_{HF} and Γ_{LF} are the high-field and low-field widths at half maximum of the first and sixth absorption lines. Estimated errors at 8 K are 2 kOe for H_{hf} and 0.01 mm/s for δ.

Sample	T (K)	$H_{hf.A}$ (kOe)	$H_{hf.B}$ (kOe)	δ_B (mm/s)	Γ_{HF} (mm/s)	Γ_{LF} (mm/s)
DG00	8	519	530	0.48	0.49	0.50
	80	519	529	0.47	0.48	0.57
	300	501	500	0.36	0.49	0.56
	450	476	465	0.27	0.52	0.68
DG10	8	516	529	0.48	0.56	0.62
	80	516	528	0.47	0.45	0.64
	300	498	499	0.36	0.46	0.70
	450	477	464	0.26	0.45	0.91
DG15	8	515	530	0.48	0.47	0.66
	80	516	529	0.47	0.47	0.77
	300	498	499	0.36	0.44	0.89
	450	473	462	0.27	0.52	1.1
DG22	8	515	531	0.47	0.46	0.70
	80	515	528	0.47	0.41	0.80
	300	498	500	0.36	0.41	0.94
	450	472	464	0.26	0.45	1.2
DG37	8	512	529	0.47	0.47	1.0
DG55	8	498	524	0.45	0.59	1.4

the data. The present results corroborate that conclusion.

As seen from Table 3 the A-site hyperfine field becomes higher than that of the B site in the vicinity of 300 K. This crossing of fields was also observed for the M samples (DA COSTA *et al.*, 1995b), as well as for Li$_{0.5}$Fe$_{2.5}$O$_4$ (YASUOKA *et al.*, 1962) and MnFe$_2$O4 (SAWATZKY *et al.*, 1969). A quantitative treatment of the temperature dependence of the hyperfine fields was carried out using the molecular field theory with the assumption of a collinear ferrimagnetic spin configuration (VANDENBERGHE and DE GRAVE, 1989). A spin of $^5\!/_2$ was attributed to Fe^{3+}, and the vacancies were restricted to B sites. The Al ions were distributed in a ratio 50/50 among the tetrahedral and octahedral sites. Example fitted curves are plotted in Fig. 6 for DG00 and DG22, and they are very similar for all four compositions. The calculated exchange integrals J_{AA}, J_{BB} and J_{AB} (see Table 4) are in remarkably good agreement with the values earlier found for the M samples. The calculated crossing temperatures, T_{invl}, increases with increasing Al content, at least up to 15 mole %.

The Curie temperatures T_C, calculated from the exchange integrals, together with the data for the M samples, are plotted as a function of the Al content in Fig. 7. The observed decrease in T_C is due to the loss of exchange paths caused by the incorporation of diamagnetic Al ions. It is seen from Fig. 7 that the present results are in agreement

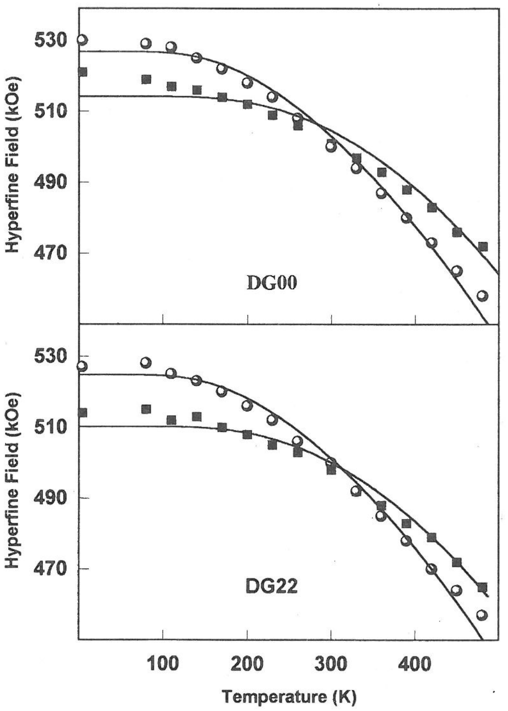

FIG. 6. Temperature dependence of the A- and B-sites hyperfine fields (squares and circles, respectively) of samples DG00 and DG22. Solid lines represent the theoretical dependence calculated using the molecular-field theory assuming a ferrimagnetic spin configuration.

Table 4. Exchange integrals J_{AA}, J_{AB}, and J_{BB}, and temperature at which $H_{hf,A}$ becomes higher than $H_{hf,B}$ (T_{invl}). All quantities are expressed in K.

Sample	J_{AA}	J_{AB}	J_{BB}	T_{invl}
DG00	−18	−27	−4	285
DG10	−16	−26	−3	298
DG15	−16	−26	−3	316
DG22	−18	−26	−4	316

with those obtained for the M samples, and a linear fit to both sets of data results in the following relations:

$$\text{DG samples: } T_C = 948 - 990y$$

$$\text{M samples: } T_C = 913 - 980y$$

The somewhat higher values for the DG samples as compared to the M samples might well be within the uncertainties (an error of 15 K would not be unreasonable) but an influence of the particle size, which is on average larger for the DG samples, cannot be ruled out.

The temperature dependences of the B-site center shifts are similar for all four DG samples, and two examples are shown in Fig. 8. The data for the A-site center shift are displaced by −0.12 mm/s. The solid curves represent the calculated variations assuming the Debye model for the lattice vibrations. The two important parameters derived from this analysis are the *characteristic Mössbauer temperature* (Θ_M) and the intrinsic isomer shift (δ_I). A conclusive variation of these two quantities with Al content could not be detected. Θ_M was found to be scattered within the range (460 ± 20) K, while a range (0.598 ± 0.006) mm/s was obtained for δ_I. These figures can be compared with the results previously reported for Al-maghemites, viz., $\Theta_M \sim 480$ K and $\delta_I \sim 0.603$ mm/s (M samples), and $\Theta_M \sim 530$ K and $\delta_I \sim 0.588$ mm/s (ML samples). These values are all typical for Fe^{3+} in oxides and oxyhydroxides (De Grave and Van Alboom, 1991).

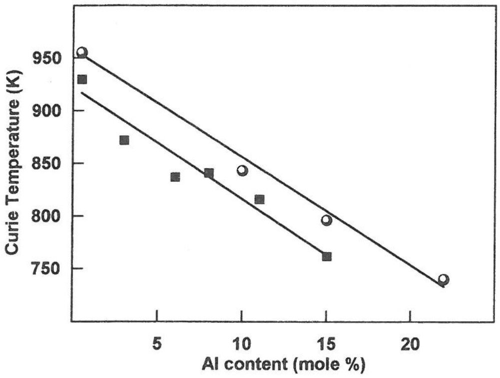

Fig. 7. Curie Temperature versus aluminum content for the DG samples (circles) and M samples (squares). Solid lines are the best linear fits to the experimental data.

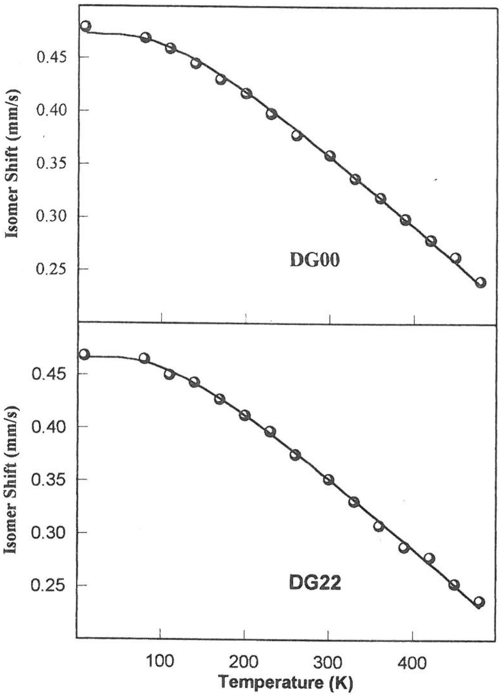

Fig. 8. Temperature dependence of the B-site isomer shift of samples DG00 and DG22. Solid lines are the calculated behavior assuming a Debye model for the lattice vibrations.

Finally, concerning the line widths, Table 3 shows that the HF widths do not change significantly with temperature or Al substitution. On the other hand, a huge broadening is noticed for the LF widths with increasing temperature, and at a given temperature, with increasing Al content. Several possible reasons for this asymmetric broadening can be enumerated (collective magnetic excitations, surface effects, inter-particle interactions, etc.) and most probably they are all operating simultaneously, thus producing highly asymmetric line shapes. For a more specific discussion in this respect, the reader is referred to an earlier paper of da Costa *et al.* (1995b).

The ZFMS of samples DG37, DG55 and DG66 at 80 K and higher display a very broad sextet component with a superimposed central doublet arising from Fe^{3+} species. For DG66 a second quadrupole doublet due to Fe^{2+} (5%, against 46% for the ferric doublet, at RT) had to be included. For obvious reasons no further attention is given to this ferrous component. It was found that a superposition of two (*i.e.* A and B sites) asymmetric sextets and doublets could not describe the experimental spectra in a proper way. Therefore, these ZFMS have been analysed with one single model-independent magnetic hyperfine field distribution (MHFD) plus a quadrupole-splitting distribution (QSD). The hyperfine field was generally chosen to vary within the range 200–550 kOe at steps of 5 kOe, and the quadrupole splitting in the range of 0–3 mm/s at steps of 0.05 mm/s. Both center shifts and line widths of the elementary sextet/doublet were adjustable. Within reasonable uncertainty limits these parameters at a given temperature were iterated to the same values for the doublet and sextet, and not significantly affected by the Al content. For the sake of comparison, the spectra of samples DG00, DG10, DG15 and DG22 at 80 K and 300 K were also fitted with this distribution approach. Some relevant parameter values for 80 K and 300 K are given in Table 5. The characteristics of the QSD profiles were not found to be affected in a relevant way by the presence of Al. The generally weak fraction of the doublet component undoubtedly prevents uncovering any significant correlation in that respect. In contrast, both the maximum-probability hyperfine field (H_{hf}^{max}) and the average hyperfine field ($\bar{H}_{hf}$) are affected by the incorporation of Al into the lattice. However, it is known that $\bar{H}_{hf}$ is strongly influenced by the fitting conditions, especially in cases where high quadrupole splitting coexist with a very broad MHFD (LE CAER *et al.,* 1984). Hence, the maximum probability hyperfine field is considered to be a more characteristic parameter, and the relations between the Al content and H_{hf}^{max} were found to be:

$$H_{hf}^{max}\ (80\ K) = (525\ -21y)\ kOe$$

$$H_{hf}^{max}\ (300\ K) = (500\ -34y)\ kOe$$

It is beyond any doubt that the external field results are the most reliable ones for the purpose of studying the effect of Al substitution. However, considering that this equipment is not available in the vast majority of the Mössbauer labs, the above equations can be used to estimate the Al content in a unknown maghemite sample, provided Al content is sufficiently high and the morphological characteristics are similar to the samples investigated in this work.

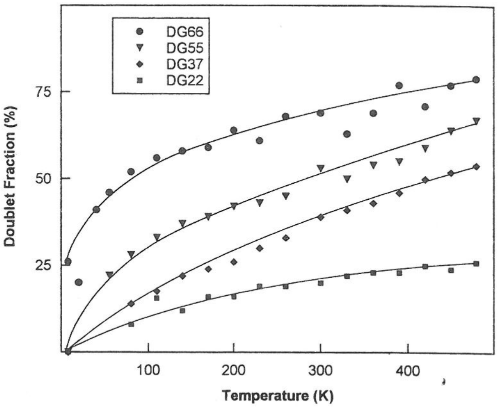

FIG. 9. Variation of the fractional area of the superparamagnetic doublet component with temperature for samples with different Al contents. Solid lines serve as a guide for the eye.

Table 5. Hyperfine parameters at 80 K and 300 K obtained from the fits with distributions of hyperfine fields and quadrupole splittings. H_{hf}^{max} and $\bar{H}_{hf}$ are the maximum probability and average hyperfine fields; σ is the square-root of the second-order moment of the distribution and δ is the center shift.

Sample	T (K)	H_{hf}^{max} (kOe)	$\bar{H}_{hf}$ (kOe)	σ (kOe)	δ (mm/s)
DG00	80	525	522	14	0.43
	300	500	496	21	0.32
DG10	80	523	518	14	0.44
	300	495	487	28	0.32
DG15	80	522	513	28	0.41
	300	494	480	33	0.32
DG22	80	519	507	34	0.42
	300	494	478	35	0.32
DG37	80	516	474	78	0.43
	300	488	407	96	0.31
DG55	80	515	444	98	0.43
	300	476	399	89	0.35
DG66	80	510	446	92	0.42
	300	480	392	88	0.30

As mentioned above, the doublet contribution to the spectra increases with increasing temperature, and this behavior is due to the existence of particles in a superparamagnetic state. The relative doublet area is plotted as a function of temperature in Fig. 9, and the temperature corresponding to a 50/50 doublet-sextet spectrum ($T_{1/2}$) can be defined from these experimental curves. The data for DG00 (no doublet at any temperature), and for DG10 and DG15 (doublets are too weak to be properly fitted) are not included in the plots. The results for samples DG37, DG55 and DG66 were obtained from the fits with a superposition of a magnetic hyperfine field distribution and a quadrupole splitting distribution. As expected, there is a steady increase of the doublet fraction with increasing Al content at any given T. The values of $T_{1/2}$ for samples DG37, DG55 and DG66 were found to be 420 K, 330 K and 70 K, respectively. It is suggested that the variations with Al are due to the concomitant effects of particle size and diamagnetic substitution. The value of $T_{1/2}$ for sample DG66 has to be considered with some caution because, as discussed previously, this sample has an impurity phase.

Another intriguing aspect reflected in Fig. 9 is the extremely broad temperature range over which mixed sextet-doublet spectra are observed. According to some authors this would indicate the absence of inter-particle magnetic interactions (Koch *et al.,* 1986; Prene *et al.,* 1993). The same phenomenon was found for the Al-free ML sample, but not for the Al-substituted members of the ML series. This remarkable behavior has remained unexplained so far, and certainly deserves further investigation.

CONCLUSIONS

The parameters derived from the external-field Mössbauer spectra collected at 4.2 K showed that at least 37 mole % Al can be incorporated into the maghemite lattice. Although an impurity in DG55 and DG66 prevents an accurate determination of the various Mössbauer parameters and of the exact Al content, there are strong indications that the maghemite phase present in those samples indeed contains more than 37 mole % Al. Thus, the apparent controversy with respect to the amount of Al that can be incorporated in maghemite seems to be related to the formation process of the investigated samples. The huge amount of data collected over the years in this laboratory for differently-prepared Al-maghemite series indeed have demonstrated that the preparation method plays a crucial role, both in the amount of Al^{3+} replacing Fe^{3+} as well as in the final characteristics of the obtained products.

Acknowledgements—This work was supported in part by the Fund for Joint Basic Research (Belgium, Grant Nr 2.0014.93), and by CNPq (Brazil).

References

Armstrong J. R., Morrish A. H. and Sawatzky G. A. (1966) Mössbauer study of ferric ions in the tetrahedral and octahedral sites of a spinel. *Phys. Lett.* **23,** 414–416.

Annersten H. and Hafner S. S. (1973) Vacancy distribution in synthetic spinel of the series Fe_3O_4-γ-Fe_2O_3. *Z. Kristallogr.* **137,** 321–340.

Bowen L. H. (1979) Mössbauer spectroscopy of ferric oxides and hydroxides. *Mössbauer Effect Data J.* **2,** 76–94.

Bowen L. H. and Weed S. B. (1984) Mössbauer spectroscopy of soils and sediments. In *Chemical Mössbauer Spectroscopy* (ed. R.H. Herber) Chap. IX, pp. 217–242. Plenum Press.

Bowen L. H., De Grave E. and Vandenberghe R. E. (1993) Mössbauer effect studies of magnetic soils and sediments. In *Mössbauer Spectroscopy Applied to Magnetism and Materials Science* (ed. G. J. Long and F. Grandjean). Vol. 1. Chap. 4. pp. 115–159. Plenum Press.

Bowen L. H., De Grave E., and Bryan A. M. (1994) Mössbauer studies in external field of well crystallized Al-maghemites made from hematite. *Hyperfine Interact.* **94,** 1977–1982.

Chadwick J., Jones D. H., Thomas M. F., Tatlock G. J. and Devenish R. W. (1986) A Mössbauer study of ferrihydrite and aluminium substituted ferrihydrites. *J. Magn. Magn. Mater.* **61,** 88–100.

Coey J. M. D. (1971) Noncollinear spin arrangement in ultrafine ferrimagnetic crystallites. *Phys. Rev. Lett.* **27,** 1140–1142.

da Costa G. M., De Grave E., Bryan A. M. and Bowen L. H. (1994a) Mössbauer studies of nano-sized aluminum-substituted maghemites. *Hyperfine Interact.* **94,** 1983–1988.

da Costa G. M., De Grave E., Bowen L. H., de Bakker P. M. A. and Vandenberghe R. E. (1994b) The center shift in Mössbauer spectra of maghemite and aluminum maghemites. *Clays Clay Minerals* **42,** 628–633.

da Costa G. M., De Grave E., Bowen L. H., de Bakker P. M. A. and Vandenberghe R. E. (1995a) Variable-temperature Mössbauer spectroscopy of nano-sized maghemite and Al-substituted maghemites. *Clays Clay Minerals* **43,** 562–568.

da Costa G. M., De Grave E., Bowen L. H., de Bakker P. M. A. and Vandenberghe R. E. (1995b) Temperature dependence of the hyperfine parameters of maghemite and Al-substituted maghemites. *Phys. Chem. Minerals* **22,** 178–185.

da Costa G. M. (1995c) Mössbauer spectroscopy and X-ray diffraction studies of maghemite (γ-Fe_2O_3) and aluminum-substituted maghemites [γ-$(Fe_{1-y}Al_y)_2O_3$] with $0 < y \leq 0.66$. Ph.D. dissertation, University of Gent.

de Bakker P. M. A., De Grave E., Vandenberghe R. E., Bowen L. H., Pollard R. J. and Persoons R. M. (1991) Mössbauer study of the thermal decomposition of lepidocrocite and characterisation of the decomposition products. *Phys. Chem. Minerals* **18,** 131–143.

De Grave E. and van Alboom A. (1991) Evaluation of ferrous and ferric Mössbauer fractions. *Phys. Chem. Minerals* **18,** 337–342.

De Grave E., Persoons R. M., Vandenberghe R. E. and de Bakker P. M. A. (1993) Mössbauer study of the high-temperature phase of Co-substituted magnetites, $Co_xFe_{3-x}O_4$. I. $x \leq 0.04$. *Phys. Rev. B* **47,** 5881–5893.

De Jesus Filho M. F., da Nova Mussel W., Qi Q. and Coey J. M. D. (1993) Magnetic properties of aluminum-doped γ-Fe_2O_3. *Proc. 6th Int. Conf. Ferrites, Tokyo 1992,* 126–128.

Eggleton R. A. and Fitzpatrick R. W. (1988) New data and a revised structural model for ferrihydrite. *Clays Clay Minerals* **36,** 111–124.

Gillot B. and Rousset A. (1990) On the limit of aluminum substitution in Fe_3O_4 and γ-Fe_2O_3. *Phys. Status Solidi (a)* **118,** K5-K8.

Haneda K. and Morrish A. H. (1977a) Vacancy ordering in γ-Fe_2O_3 small particles. *Solid State Commun.* **22,** 779–782.

Haneda K. and Morrish A. H. (1977b) On the hyperfine field of γ-Fe_2O_3 small particles. *Phys. Lett.* **64A,** 259–262.

Hendriksen P. V., Linderoth S., Oxborrow C. A. and Mørup S. (1994a) Ultrafine maghemite particles: II. The spin-canting effect revisited. *J. Phys.Condens. Matter* **6,** 3091–3100.

Hendriksen P. V., Bødker F., Linderoth S., Wells S. and Mørup S. (1994b) Ultrafine maghemite particles: I. Studies of induced magnetic texture. *J. Phys.Condens. Matter* **6,** 3081–3090.

Koch J. W. C., Madsen M. B. and Mørup S. (1986) Decoupling of magnetically interacting crystallites of goethite. *Hyperfine Interact.* **28,** 549–552.

Klug H. P. and Alexander L. E. (1974) *X-ray Diffraction Procedures for Polycrystalline and Amorphous Materials.* John Wiley and Sons.

le Caer G., Dubois J. M., Fischer H., Gonser U. and Wagner H. G. (1984) On the validity of ^{57}Fe hyperfine field distribution calculation from Mössbauer spectra of magnetic amorphous alloys. *Nucl. Instr. Methods* **B5,** 25–33.

Morrish A. H., Haneda K. and Schurer P. J. (1976) Surface magnetic structure of small γ-Fe_2O_3 particles. *J. de Phys.* **37,** C6301–305.

Mørup S. and Topsøe H. (1976) Mössbauer studies of thermal excitations in magnetically ordered microcrystals. *Appl. Phys.* **11,** 63–66.

Pollard R. J. (1990) The spin canting anomaly in ferrimagnetic particles. *J. Phys. Condens. Matter.* **2,** 983–991.

Pollard R. J. and Morrish A. H. (1987) High-field magnetism in non-polar γ-Fe_2O_3 recording particles. *IEEE Trans. Magn.* **23,** 42–44.

Prene P., Tronc E., Jolivet J. P., Livage J., Cherkaoui R., Nogues M., Dormann J. L. and Fiorani D. (1993) Magnetic properties of isolated γ-Fe_2O_3 particles. *IEEE Trans. Magn.* **29,** 2658–2660.

Rousset A. and Paris J. (1972) Formation des solutions solides binaires et ternaires des sesquioxydes de chrome, d'aluminium et de fer III- Le systeme Fe_2O_3-Al_2O_3. *Bull. Soc. Chim.* **10,** 3729–3733.

Rousset A., and Paris J. and Chassagneux F. (1979) Interet de la reactivite des solides pour l'obtention de phases nouvelles. *Ann. Chim. Fr.* **4,** 115–122.

Sawatzky G. A., van der Woude F. and Morrish A. H. (1969) Mössbauer study of several ferrimagnetic spinels. *Phys. Rev.* **187,** 747–757.

Schwertmann U., and Fechter H. (1984) The influence of aluminum on iron oxides: XI. Aluminum-substituted maghemite in soils and its formation. *Soil Sci. Soc. Am. J.* **48,** 1462–1463.

Vandenberghe R. E., Vanleerberghe R., De Grave E. and Robbrecht G. (1980) Preparation and magnetic properties of ultra-fine cobalt ferrites. *J. Magn. Magn. Mater.* **15–18,** 1117–1118.

Vandenberghe R. E. and De Grave E. (1989) Mössbauer Studies of Oxidic Spinels. In *Mössbauer Spectroscopy Applied to Inorganic Chemistry* (ed. G. J. Long and F. Grandjean). Vol. 3. Chap. 3, pp 59–182. Plenum.

Vandenberghe R. E., De Grave E. and de Bakker P. M. A. (1994) On the methodology of the analysis of Mössbauer spectra. *Hyperfine Interact.* **83,** 29–49.

van Oosterhout G. W. and Rooijmans C. J. M (1958) A new superstructure in gamma-ferric oxide. *Nature* **181,** 44.

Wolska E. and Schwertmann U. (1989) The vacancy ordering and distribution of aluminium ions in γ-$(Fe,Al)_2O_3$. *Solid State Ionics* **32/33,** 214–218.

Yasuoka H., Hirai A., Matsuura M. and Hashi T. (1962) Hyperfine field at ^{57}Fe in lithium ferrite measured by NMR. *J. Phys. Soc. Japan* **17,** 1071–1072.